European Journal of Medicinal Chemistry 58 (2012) 368–376

Contents lists available at SciVerse ScienceDirect

European Journal of Medicinal Chemistry

journal homepage: http://www.elsevier.com/locate/ejmech

Original article

Design, synthesis and biological evaluation of 5-hydroxy, 5-substituted-pyrimidine-2,4,6-triones as potent inhibitors of gelatinases MMP-2 and MMP-9

Orazio Nicolotti**, Marco Catto, Ilenia Giangreco, Maria Barletta, Francesco Leonetti, Angela Stefanachi, Leonardo Pisani, Saverio Cellamare, Paolo Tortorella, Fulvio Loiodice, Angelo Carotti*

Dipartimento di Farmacia, Università degli Studi di Bari "Aldo Moro", via Orabona 4, I-70125 Bari, Italy

ARTICLE INFO

Article history:
Received 2 July 2012
Received in revised form
7 September 2012
Accepted 25 September 2012
Available online 5 October 2012

Keywords:
MMP
Gelatinases
ZBG
QSAR
Molecular docking

ABSTRACT

Matrix metalloproteinases (MMPs) are attractive biological targets that play a key role in many physiopathological processes such as degradation of extracellular matrix proteins, release and cleavage of cell-surface receptors, tumour progression, homeostatic regulation and innate immunity. A series of 5-hydroxy, 5-substituted pyrimidine-2,4,6-triones were rationally designed, prepared and tested as inhibitors of gelatinases MMP-2 and MMP-9 and collagenase MMP-8. On one side, the presence of the 5-hydroxyl group, that represents an typical feature of this class of compounds, ensured an attractive pharmacokinetic profile while on the other suitably substituted biaryl molecular fragments, attached to position 5 through a ketomethylene linker, guaranteed favourable interaction in the deep region of the S_1' enzymatic subsite. This rational design led to the discovery of highly potent MMP inhibitors. In particular, biphenyl derivatives bearing at the *para* position $COCH_3$ and OCF_3 substituents permitted to inhibit gelatinases MMP-2 and MMP-9, with IC_{50} values as low as 30 nM and 21 nM, respectively, whereas the introduction at the same position of the bulkier SO_2CH_3 group afforded a potent collagenase MMP-8 inhibitor with an IC_{50} value equal to 66 nM. Molecular docking simulations allowed us to elucidate key interactions driving the binding of the top active compounds towards their preferred MMP target.

1. Introduction

The great interest towards matrix metalloproteinases (MMPs), a family of zinc- and calcium-dependent endopeptidases, stems from their primary role in the degradation of the extracellular matrix (ECM) [1]. Overexpression and/or misregulation of MMPs may trigger various inflammatory, malignant, and degenerative diseases [2–5]. Selective MMP inhibition is therefore an important goal in medicinal chemistry research to tackle severe and widespread diseases [6,7].

MMP-2 and MMP-9 have a relevant role in the pathogenesis of cancer, heart disease and inflammation and indeed the major focus of the present investigation was the inhibition of these two gelatinases characterized by fibronectin-like inserts enabling them to bind and process gelatine. Nowadays, a high number of orally available broad-spectrum MMP inhibitors (MMPIs) have been identified. Most of them contain the hydroxamate function, which strongly interacts with the zinc ion in the MMP catalytic site, and thus are often non selective compounds. Moreover, concerns have been raised about the true clinical efficacy and significant toxicity of this class of MMP inhibitors [8]. As a result, increasing attention has been paid to the identification of new zinc binding groups (ZBGs) that could represent a valuable alternative to the hydroxamate function [9–13].

In this context, our effort has been devoted to the design of novel barbiturate derivatives to be further developed as potent MMPIs. A large number of 5,5-disubstituted pyrimidine-2,4,6-triones, exhibiting high affinities over several MMP subtypes [14–17], has been already reported and more recently they have been studied also as putative radiotracers to non-invasively locate activated MMPs by means of positron emission tomography (PET) [18,19]. Moreover, the very attractive drug-likeness [20] of barbiturates compared to hydroxamates makes them good starting structures for the design of more promising and safer MMPIs. In this respect, the need of achieving a good balance between binding potency and pharmacokinetic properties prompted us to insert at the C5 carbon two quite different substituents, one belonging to

* Corresponding author. Tel.: +39 080 5442782; fax: +39 080 5442230.
** Corresponding author. Tel.: +39 080 5442551; fax: +39 080 5442230.
E-mail addresses: orazio.nicolotti@uniba.it (O. Nicolotti), angelo.carotti@uniba.it (A. Carotti).

0223-5234/$ – see front matter © 2012 Elsevier Masson SAS. All rights reserved.
http://dx.doi.org/10.1016/j.ejmech.2012.09.036

a series of variously decorated biphenyl arms to explore the binding interactions at the S_1' subsite while the other was a hydroxyl group to modify hydrophobic properties and ensure a fair pharmacokinetic profile, quite diverse from the barbiturates explored so far carrying generally two highly hydrophobic substituents at position 5.

Our molecular design was also inspired by findings from an our recent paper [21], where we have examined a number of ZBGs (e.g., barbiturates, hydroxypyrones and hydroxypyridinones) and their potential in biasing selectively MMPs [22]. In particular, we described how the chelation of the catalytic zinc ion by the pyrimidine-2,4,6-trione ring could be further reinforced by the specific occurrence of additional interactions, including hydrogen bonds and van der Waals (vdW), that may determine a consistent gain of molecular affinity and selectivity [21]. Originally, such a study started from the analysis of our electronic database archiving a wealth of physicochemical and biochemical information of a molecular library containing >2000 chemicals prepared in our laboratories [21,23] that led us to find a number of 5-hydroxy, 5-substituted-pyrimidine-2,4,6-triones prepared as chemical intermediates for the synthesis of pyrimido[4,5-c]pyridazine inhibitors of monoamine oxidases [24]. Given the weak activity towards MMPs measured for the fished hits (**1**–**4** of Table 1), the phenyl moiety of such compounds was augmented to biphenyl, a privileged fragment for targeting the S_1' subsite of MMPs. In agreement with previous findings, this knowledge-based approach has permitted to obtain a number of compounds (i.e., **5**, **6** and **16**) inhibiting the gelatinases MMP-2 and MMP-9 and to a lesser extent the collagenase MMP-8. The binding interactions of inhibitors **5**, **6** and **16** have been deeply investigated by means of molecular dynamics (MD) simulations and free energy perturbation calculations [21]. The encouraging binding affinity observed for the *para*-carboxamido analogue (**16**; IC_{50} = 87 nM at MMP-2) prompted us to further explore the *para* position with a series of substituents spanning a wider chemical space in terms of Hammett σ and Hansch π substituent constants [25]. Satisfactorily, our approach led to the discovery of additional interesting compounds with inhibitory activity towards MMP-2 comparable to or higher than reference compound **16** and remarkably increased towards MMP-9. Besides the *para* position, other structural variations were made to explicitly target other sensitive enzymatic regions. Quantitative structure–activity relationships and docking studies allowed the identification of the main molecular determinants responsible for the high affinity showed by our derivatives.

Table 1
MMP-2, MMP-9 and MMP-8 inhibitory activities of compounds **1**–**20**.

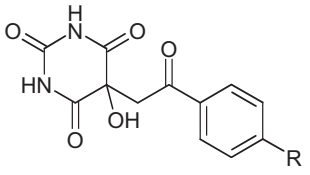

Entry	R	Gelatinases		Collagenase
		MMP-2[a]	MMP-9[a]	MMP-8[a]
1[b]	H	(0%)	44,200 ± 1600	42,900 ± 700
2[b]	CF_3	39,000 ± 700	(11%)	8200 ± 100
3[b]	OCH_3	21,200 ± 400	13,000 ± 400	6800 ± 900
4[b]	NO_2	(0%)	(8%)	63,000 ± 1000
5[b]	C_6H_5	184 ± 24	517 ± 10	266 ± 36
6[b]	C_6H_4-3′-Cl	60,000 ± 4000	19,800 ± 3100	4500 ± 100
7	C_6H_4-3′-NO_2	8100 ± 900	27,500 ± 14,800	2600 ± 800
8	C_6H_4-4′-CH_3	301 ± 13	103 ± 30	336 ± 37
9	C_6H_4-4′-Cl	278 ± 26	66 ± 12	271 ± 43
10	C_6H_4-4′-CH_2OH	148 ± 40	561 ± 82	210 ± 8
11	C_6H_4-4′-OCH_3	121 ± 47	141 ± 16	184 ± 42
12	C_6H_4-4′-OCF_3	143 ± 3	21 ± 1	715 ± 100
13	C_6H_4-4′-SCH_3	120 ± 8	86 ± 27	313 ± 38
14	C_6H_4-4′-SO_2CH_3	58 ± 2	650 ± 120	66 ± 11
15	C_6H_4-4′-$COCH_3$	30 ± 1	170 ± 30	109 ± 20
16[b]	C_6H_4-4′-$CONH_2$	87 ± 24	1800 ± 210	586 ± 91
17	C_6H_4-4′-$CON(CH_3)_2$	1340 ± 60	3010 ± 650	2020 ± 270
18	Thien-3-yl	181 ± 8	159 ± 24	153 ± 23
19	[c]	10%[d]	21%[d]	26%[d]
20	[c]	38%[d]	28%[d]	71%[d]

[a] Inhibition data are expressed as IC_{50} (nM) ± SEM or % inhibition at 10 μM (in parentheses) from 2 or 3 different experiments.
[b] Data reported in Ref. [21].
[c] Structures in Scheme 1b.
[d] % inhibition at 100 μM concentration.

2. Results

2.1. Chemistry

5-Hydroxy, 5-substituted pyrimidine-2,4,6-triones were prepared via aldol addition of suitable methyl ketones to pyrimidine-2,4,6-trione (i.e., alloxan) as already described [24]. When not commercially available, substituted biaryl methyl ketones **I** were prepared via microwave assisted Suzuki–Miyaura reaction of 4-bromoacetophenone and arylboronic acids (Scheme 1a). Reaction of alloxan hydrate with biaryl methyl ketones **I** yielded comps **7**–**15**, **17** and **18** (Scheme 1a) whereas a mixture of isomeric compounds **19** and **20** was obtained in the reaction with biphenyl acetone (Scheme 1b).

Biological assays. MMP-2, -8, -9 inhibitory activities were determined by a fluorimetric assay, where a pro-fluorescing peptide was used as substrate, and the fluorogenic activity of its cleavage product was measured after coincubation with MMP of the tested compounds.

2.2. Molecular modelling studies

The program GOLD 5.1 was used in all the docking simulations [26]. In the present investigation, GOLD returned a confident reliability as it well reproduces the binding conformation of different molecules co-crystallized with MMP proteins. As a measure of fit, the rmsd value was calculated over all the heavy atoms between the docking pose and the X-ray conformation of ligands in complex with the two gelatinases MMP-2 (pdbcode 1HOV) and MMP-9 (pdbcode 2OVX) and the collagenase MMP-8 (pdbcode 1I73) and deviations as small as 1.04 Å, 1.24 Å and 1.70 Å, were observed.

The program QikProp (QikProp, version 3.4, Schrödinger, LLC, New York, NY, 2011) was used to predict a number of pharmaceutically relevant properties (e.g., octanol/water partition coefficient, log P; aqueous solubility, log S; and binding to human serum albumin, log Khsa) for five reference compounds [14,17,18,20] in comparison with inhibitors **5**, **8**–**17** of Table 1. As a measure of goodness, the interested user can assess the high concordance between measured (5.6×10^{-4} g/mL) and predicted (4.3×10^{-4} g/mL) aqueous solubility for a compound elsewhere described [20].

3. Results and discussion

The need of discovering novel ZBG-containing compounds prompted us to first interrogate our electronic database storing a chemical library of >2000 rationally designed biological active compounds synthesized since late eighties in the laboratories of our group. As shown in Fig. 1, the likelihood of our library to exhibit activity in any therapeutic area has been estimated by comparing its bioactive profiles (i.e., distribution of physical properties relevant for

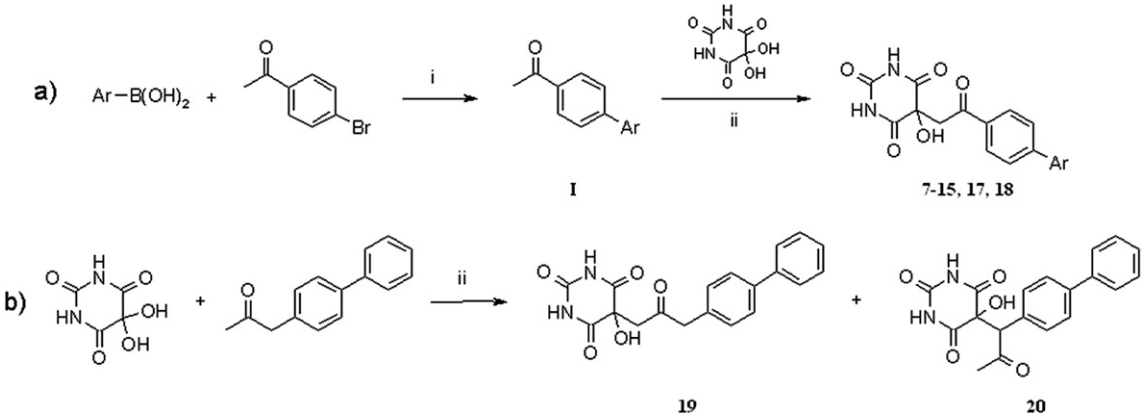

Scheme 1. *Reagents and conditions*: (i) Na_2CO_3, $(PPh_3)_2PdCl_2$, water/dioxane, microwave heating; (ii) acetic acid, reflux.

druglikeness such as molecular weight, log P, number of hydrogen bond donor atoms and number of hydrogen bond acceptor atoms) with those derived from DrugBank [27], a freely available database containing FDA-approved small molecule drugs, FDA-approved biotech drugs, nutraceuticals and experimental drugs.

Interestingly, besides a large series of compounds bearing canonical ZBGs (i.e., carboxylic acids and thiols), four original 5,5-disubstituted pyrimidine-2,4,6-triones have been also fished as potential hits. The rationale behind such a selection has been based on previously reported studies available in the literature [14–19]. Our attention has been focused on the 5-OH group featuring these compounds because of its potential role in determining a more appropriate hydrophilic/lipophilic balance and in engaging HB interactions. In this respect, the four 5,5-disubstituted pyrimidine-2,4,6-triones retrieved from our collection have been submitted to docking calculations, and the plausible binding poses found in the MMP-2 enzyme increased our confidence in raising up these compounds as MMP-2 inhibitors [21]. Interestingly, biological experimental data awarded a number of these selected derivatives (**1**–**4**; Table 1) with MMP inhibition potency in the high micromolar range. The inhibitory potency of the selected pyrimidine-2,4,6-trione derivatives has been then improved through a knowledge-based molecular design rooted on the elementary concept of assembling the pyrimidine-based core with a biphenyl arm, a fragment widely used to target the S_1' subsite of MMPs. Our efforts resulted three barbiturate-based derivatives (**5**, **6** and **16**; Table 1 [21]) with two of them showing interesting binding potential towards MMPs. In that investigation, our attention has been mostly paid to interpret, via MD and free energy perturbation techniques, the dramatic difference of the binding affinities towards MMP-2 between compounds **6** and **16**, IC_{50} 60,000 *vs*. 87 nM, respectively, despite a slight structural change. The interested reader is referred to elsewhere for a complete description [21].

In the present study, we prefer to better explore the *para* position of the biphenyl ring with the purpose to improve potency towards MMP-2 while minor emphasis has been placed at this stage in studying the substituent changes at the *meta* position given the disappointing results recently obtained by compound **6**. In

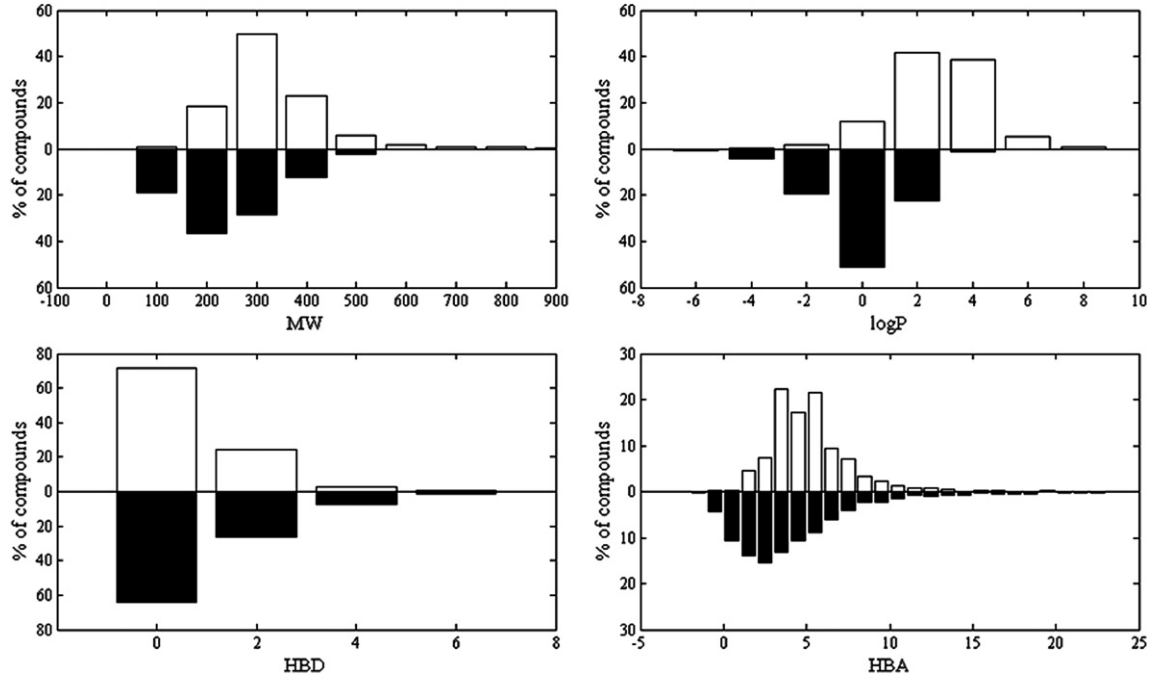

Fig. 1. The physical property profiles of our academic collection (in black) are compared with property profiles found in DrugBank (in white). The *y*-axis represents the percentage of compounds, the *x*-axis represents the molecular weights (MW), log P, hydrogen bond donor (HBD) and hydrogen bond acceptors (HBA) profiles.

doing so, we prepared a panel of variously substituted barbiturate-based derivatives (**7**–**15** and **17**) by decorating the distal phenyl ring with selected functional groups having easy commercial and chemical access as well as different Hammett σ and Hansch π substituent constants. Finally, isosteric 3-thienyl derivative **18** was also prepared along with two additional derivatives **19** and **20** carrying longer and branched biphenyl-containing molecular fragments at position 5, respectively. For the sake of completeness, data for derivatives **1**–**6** and **16** already described in our recent work [21] are also listed in Table 1.

As shown in the Craig plot in Fig. 2, the physicochemical landscape was fairly explored changing the σ and π coordinates by selecting a pool of suitable substituents. In particular, a number of easily accessible functional groups was chosen to assess their effect in targeting MMPs. Interestingly, it was observed that MMP-2 inhibitory activity is benefited by the presence of electron withdrawing groups (EWG) while the hydrophobic effects are less relevant although low values of π are to some extent welcome. The shift from the *para*-$CONH_2$ (**16**) to the *para*-$COCH_3$ (**15**) EWG resulted an increase of affinity towards MMP-2 from 87 to 30 nM IC_{50} likely due to an increment of σ from 0.36 to 0.50. Similarly, changing the *para*-$CONH_2$ (**16**) to the *para*-SO_2CH_3 EWG (**14**) improved affinity towards MMP-2 from 87 to 58 nM following a variation of the σ value from 0.36 to 0.72. On the other hand, the replacement of *para*-$CONH_2$ (**16**) EWG with a *para*-OCH_3 electron donor groups (EDG) (**11**) had a detrimental impact on the affinity towards MMP-2. Focussing on parent compound and *para* derivatives (**5**, **8**–**17**), some linear tendency emerged by relating binding affinity towards MMP-2 with both σ and π constants, as follows:

$$pIC_{50,MMP-2} = 6.82(\pm0.09) + 0.458(\pm0.28)\sigma_p - 0.116(\pm0.09)\pi$$
$$s = 0.237 \quad n = 10 \quad r^2 = 0.520 \qquad (1)$$

In this and in the following equations, s, n and r^2 represent the standard deviation, the number of the examined compounds and the squared correlation coefficient, respectively. Normally, a negative coefficient with π constant would indicate unfavourable interactions in a non-hydrophobic or polar local environment [28]. In these cases, as amply demonstrated in past QSAR studies [29–33], the use of the MR, that is the substituent molar refractivity [25], allows to deriving more solid and interpretable QSAR models.

Actually, the replacement of π with MR in equation (1) yielded equation (2) having slightly improved statistical parameters.

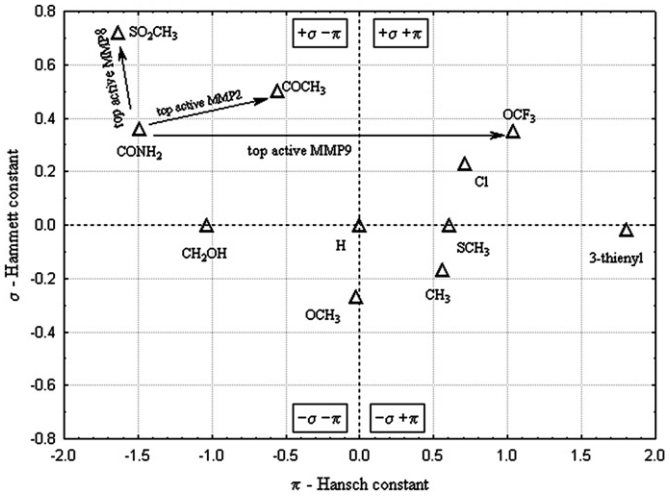

Fig. 2. Choice of substituents at the *para* position of the biphenyl fragment by multidimensional mapping based on the Hammett (σ) and Hansch (π) constants.

$$pIC_{50,MMP-2} = 6.55(\pm0.18) + 0.404(\pm0.28)\sigma_p + 0.350(\pm0.22)MR$$
$$s = 0.225 \quad n = 10 \quad r^2 = 0.565 \qquad (2)$$

However, despite the poor statistics recommended great caution, equation (2) seemed to suggest the occurrence of polar interactions in a non-hydrophobic enzymatic region, accounted for by MR, whose strength is favoured by the EWG character of the *para* substituents, as assessed by σ (*vide infra*).

A clearer and more consistent trend was observed when modelling the MMP-9 binding affinity that, more specifically, benefited of the presence of EWG with more pronounced hydrophobic character. In this respect, the most active compounds were those combining high values for both σ and π substituent constants. Striking examples are the *para*-OCF_3 (**12**) and the *para*-Cl (**9**) derivatives inhibiting MMP-9 with IC_{50} values equal to 21 and 66 nM, respectively. Interestingly, the multivariate analysis of inhibition data from parent compound and *para* derivatives (**5**, **8**–**17**) returned the following informative equation:

$$pIC_{50,MMP-9} = 6.73(\pm0.09) + 0.504(\pm0.29)\sigma_p + 0.617(\pm0.10)\pi$$
$$s = 0.243 \quad n = 10 \quad r^2 = 0.861 \qquad (3)$$

showing a high r^2 and even a confident value of q^2, that is the square correlation coefficient for prediction from the *leave-one-out* procedure [34], as high as 0.738. Importantly, equation (3) explicitly indicated the occurrence of favourable lipophilic interactions of the *para*-substituents in the MMP-9 binding site.

Interestingly, this binding hypothesis and the additional information coming from the QSAR equations were further confirmed and complemented by the analysis of the structural features of the MMP-2 and MMP-9 binding sites, in particular the S_1' subsite [35], and, more importantly, by docking simulations of selected inhibitors into their binding pockets.

The informative QSAR models obtained for gelatinases MMP-2 and MMP-9 prompted us to extend the investigation to the MMP-8, which is instead a member of the collagenases. Unfortunately, the examination of the same series of *para* derivatives did not furnish a clear picture of the physicochemical forces driving the inhibitors binding to MMP-8. Given the uneven distribution and narrow spread of pIC_{50} values, very disappointingly, a poor correlation ($r^2 < 0.250$) was observed by using the same substituents parameters applied for modelling MMP-2 and MMP-9 inhibitory activities in equations (1)–(3).

To further extend our structure–activity relationship study, three more compounds were designed, prepared and tested. As the isosteric substitution of one phenyl with a 3-thienyl ring in a biphenyl moiety was successfully applied to HDAC inhibitors affording much more potent compounds [36,37], the same replacement was made on lead compound **5** affording compound **18**. Very satisfactorily, this compound exhibited an equal inhibitory potency at MMP-2 and a significantly higher potency at both MMP-9 and MMP-8 compared to the phenyl isoster **5**.

To better explore the binding region around the 5 position of the pyrimidine-2,4,6-trione scaffold, two new compounds, that is compounds **19** and **20** in Table 1, were designed and contemporarily prepared through the single reaction reported in Scheme 1b. Compound **19** was conceived to increase the length and the conformational mobility of the biaryl arm whereas compound **20** to look for additional favourable interactions around the keto-methylene group. Unfortunately, both compounds displayed very weak inhibition towards the three tested MMPs (Table 1).

Docking studies were undertaken to identify at a 3D level the driving forces governing the interaction [38,39] at the MMP binding sites of our inhibitors. Initial coordinates for the two gelatinases,

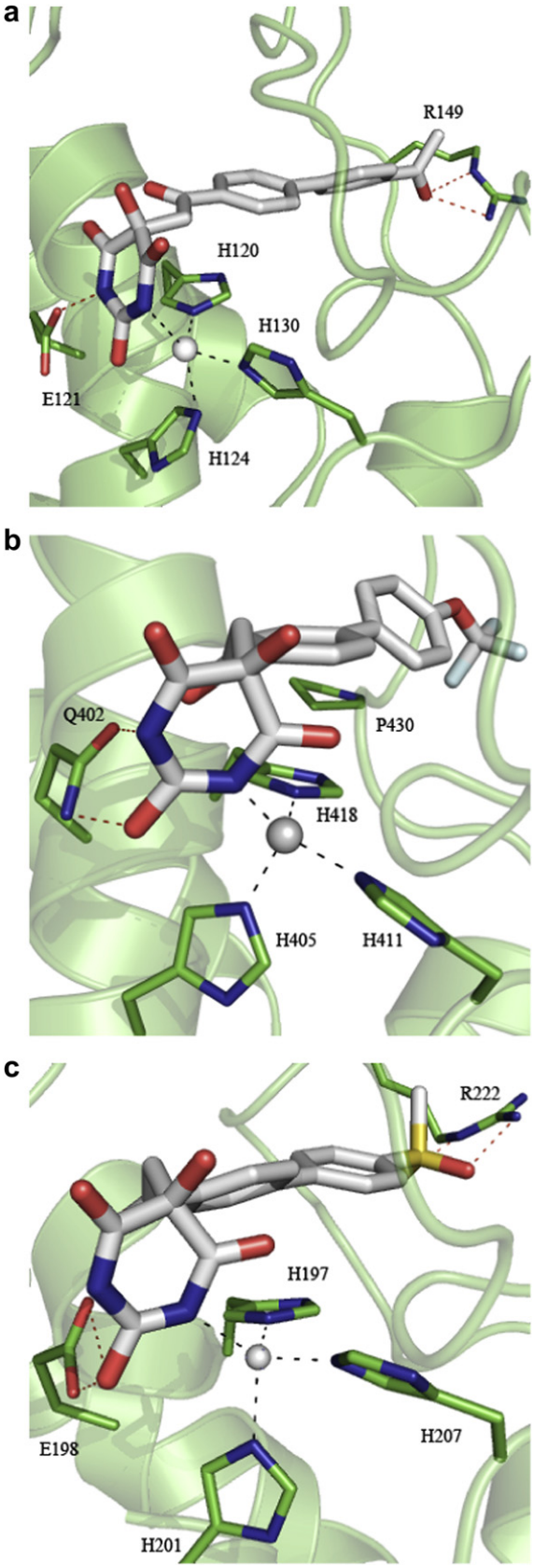

MMP-2 and MMP-9, were taken from structural models deposited in the Protein Data Bank (PDB) with the entry code 1HOV and 2OVX, respectively. The PDB entry 1I73 was instead selected for docking studies of the collagenase MMP-8. A wealth of information was gathered by inspecting other available PDB structures of MMPs complexed with barbiturate inhibitors [40,41]. On this basis, a model where the N1 atom of the barbiturate coordinates the metal ion with a tetrahedral geometry, and the oxygen atom interacts via an HB with the side chain of Glu121 (numbering as in 1HOV) has been accepted as the most reasonable. As a result, the enolic form of the barbiturate is supposed to be the favoured tautomer in protein context over the keto form that is instead prevalent in solution [42]. An additional HB is observed between carbonyl oxygen atom of C4 and Ala84 (numbering as in 1HOV) that is part of the conserved AHA motif S_1 of the MMP binding site [43,44]. As described in Fig. 3a, the docking pose of the most active compound **15** ($IC_{50} = 30$ nM) into the MMP-2 active site showed that the barbiturate core acted indeed as ZBG. In particular, the N1 atom ensured the coordination to the zinc ion by assuming, along with the three catalytic histidine residues, a tetrahedral geometry, while the charged Glu121 residue was engaged in HB with the N3 atom located at a distance of 2.7 Å. As expected, the *para*-$COCH_3$ biphenyl arm was buried into the S_1' subsite where determinant HBs were established between the oxygen atom of the acetyl substituent and guanidine groups of and Arg149 residue. A scoring value as high as −71.88 kJ/mol was estimated when docking compound **15**. Despite the E121Q variation (1HOV numbering), a similar posing (Fig. 3b) was observed when docking the highest active compound **12** ($IC_{50} = 21$ nM) into the MMP-9 active site and a comparable value of scoring equal to −69.32 kJ/mol was in fact observed. However, the comparison between the S_1' subsites of MMP-2 and MMP-9 disclosed an important residue change (from arginine to proline at position 149; 1HOV numbering) [45]. As a result, the binding at MMP-9 could be mainly driven by hydrophobic interactions at the S_1' subsite. Interestingly, such information confirmed what already emerged in the 2D QSAR analysis (equation (3)) indicating the positive influence of hydrophobic groups ($\pi > 0$) at the *para* position on the MMP-9 affinity.

Finally, the docking pose of the highest active compound **14** ($IC_{50} = 66$ nM) into the MMP-8 active site is reported in Fig. 3c. As can be seen, no appreciable differences were discernable in the way the barbiturate scaffold binds the zinc ion. Importantly, the anchoring of the bulkier *para*-SO_2CH_3 substituent into the deeper region of the S_1' subsite was assured by the formation of an HB with Arg222 of MMP-8 with scoring value equal to −81.89 kJ/mol.

Besides our efforts in the design of optimal biphenyl arm engaging S_1' subsite, we kept an open eye on the evaluation of a number of pharmaceutically relevant properties (e.g., octanol/water partition coefficient, log P; aqueous solubility, log S; and binding to human serum albumin, log Khsa). To this aim, we used QikPro to predict such properties for inhibitors **5**, **8**–**17** in Table 1 as well as for five structurally close barbiturate derivatives retrieved by recent literature [14,17,18,20] and used as reference compounds. As can be seen in Fig. 4a–c, the presence of the hydroxyl group at C5 that is a unique feature of compounds **5**, **8**–**17** compared to reference literature compounds might improve the lipophilic–hydrophilic-balance, increase the aqueous solubility and reduce the binding to human serum albumin with a likely significant gain in terms of bioavailability.

Fig. 3. Zoomed in view of main interactions of top active compounds **15**, **12** and **14** (coloured in white) at the protein binding sites, rendered as cartoon models, of MMP-2 (a), MMP-9 (b) and MMP-8 (c), respectively. For the ease of interpretation, key residues are represented as ball and stick while black and red dashed lines represent the coordination to the catalytic zinc ion and hydrogen bonds, respectively. (For interpretation of the references to colour in this figure legend, the reader is referred to the web version of this article.)

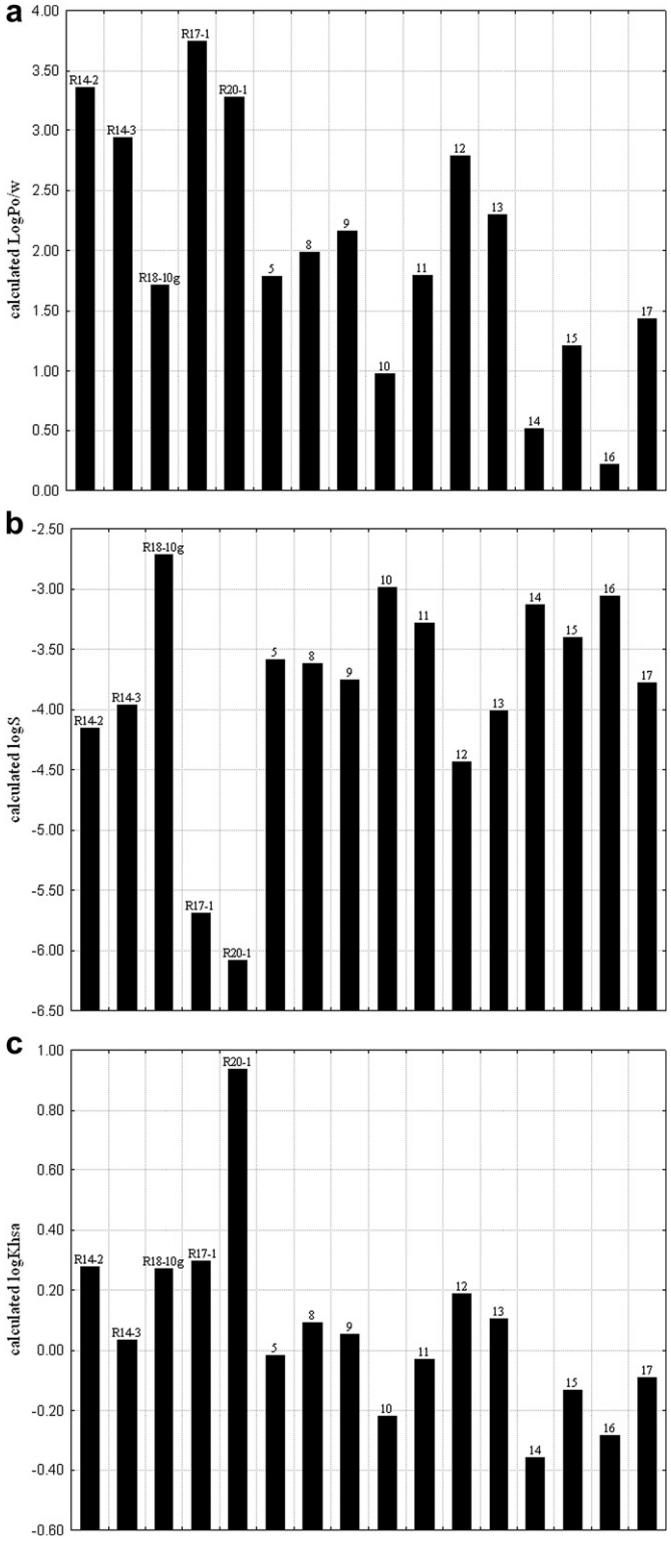

Fig. 4. Histograms describing the variation of some calculated pharmaceutically relevant properties that are: (a) octanol/water partition coefficient, log P; (b) aqueous solubility, log S; and (c) binding to human serum albumin, log Khsa. The first five bars are referred to compounds retrieved by recent literature where the letter R indicates the corresponding endnote [14,17,18,20] and the digit the numbering of the original paper (see also Supplementary Materials). The remaining bars are related with inhibitors **5**, **8**–**17** in Table 1 as indicated by the reported labels.

4. Conclusions

The basic idea behind our current investigation was the repurposing of properly modified pyrimidine-2,4,6-triones as MMP inhibitors to avoid the unwanted properties of hydroxamate MMP inhibitors while ensuring more attractive drug-likeness. In this respect, we tried to achieve a better pharmacokinetic profile by inserting as a substituent at the C5 a hydroxyl group, which ensured a better log P, an improved aqueous solubility and a limited binding to human serum albumin as well. On the other hand, the second substituent of the C5 was chosen by using a pool of variously decorated biphenyl moieties having diverse hydrophobic, electronic and steric properties to explore the chance of interactions at the S_1' subsite. The good inhibition data obtained suggested that our compounds merit further exploration (especially as selective gelatinase inhibitors) [46]. And in fact, the design of novel MMP-2 inhibitors is still an open challenge in medicinal chemistry research.

5. Experimental section

5.1. Chemistry

Syntheses of biaryl methyl ketones intermediates **I** and compounds **7**–**15** and **17**–**20** were performed using a Milestone Microsynth oven, and a Büchi Syncore parallel reactor, respectively. Commercial reagents and solvents were purchased from Sigma–Aldrich Europe. Melting points (mp) were taken on a Gallenkamp MFB 595010 M apparatus and are uncorrected. Elemental analyses were performed on a EuroEA 3000 analyser for C, H, N; experimental results agreed to within ±0.40% of the theoretical values. ESI mass spectra (not reported) were performed on a Agilent 1100 series LC-MSD trap system VL apparatus. ^{1}H NMR spectra were recorded in DMSO-d_6, unless otherwise stated, on a Varian Mercury 300 spectrometer. Chemical shifts are expressed in δ (ppm) and the coupling constants J in Hz. The following abbreviations were used: s, singlet; d, doublet; t, triplet; m, multiplet. Exchange with deuterium oxide was used to identify OH and NH protons. Chromatographic separation of isomer compounds **19** and **20** was performed on a Biotage SP1 purification system using flash cartridges pre-packed with KPSil™ 32–63 μm, 60 Å silica.

5.1.1. Synthesis of biaryl methyl ketones *I*

In a sealed microwave vessel equipped with magnetic stirrer and optical sensor for temperature detection, 1.0 mmol of 4-bromoacetophenone (0.20 g), 1.2 mmol of opportune phenylboronic acid, 0.05 mmol of dichlorobis(triphenylphosphine)palladium(II) (0.04 g) and 3.0 mmol of sodium carbonate (0.32 g) were suspended in 3 mL of dioxane and 3 mL of water. Microwave heating was set as follows: 800 W, ramping from room temperature (rt) to 150 °C in 3 min, heating at 150 °C for 10 min, then cooling to rt. The residue was filtered, washed with diethyl ether and dried as white precipitate. All biaryl methyl ketones **I** were characterized by their LC–MS and ^{1}H NMR spectra and used without further purification; yields 62–81%.

5.1.2. Synthesis of compounds *7*–*15* and *17*–*20*

0.5 mmol of alloxan monohydrate (0.08 g) and suitable methyl ketone were suspended in 5 mL of glacial acetic acid and reacted in a Syncore apparatus set at the temperature of 115 °C, shaking at 120 rpm and reaction time 3 h. All the targeted compounds precipitated after cooling and were recrystallized from ethanol.

Compounds **19** and **20** were obtained as a mixture in a 36:64 ratio (total yield 75%); chromatographic purification of the crude (gradient eluent: methanol in dichloromethane 0–10%) afforded the pure final compounds.

*5.1.2.1. 5-[2-(3′-Nitrobiphen-4-yl)-2-oxoethyl]-5-hydroxy-hexahydropyrimidine-2,4,6-trione (**7**).* 64% Yield, mp 246–8 °C ^{1}H NMR δ 11.46 (s, 2H, NH), 8.51 (s, 1H), 8.21–8.29 (m, 2H), 8.09 (d, 2H, $J_o = 8.1$), 7.96 (d, 2H, $J_o = 8.1$), 7.79 (t, 1H, $J_o = 8.1$), 7.33 (s, 1H, OH), 3.95 (s, 2H). Anal. % ($C_{18}H_{13}N_3O_7$) calculated: C 56.40, H 3.42, N 10.96; found C 56.28, H 3.37, N 10.68.

*5.1.2.2. 5-[2-(4′-Methylbiphen-4-yl)-2-oxoethyl]-5-hydroxy-hexahydropyrimidine-2,4,6-trione (**8**).* 69% Yield, mp > 250 °C ^{1}H NMR δ 11.46 (s, 2H, NH), 8.02 (d, 2H, $J_o = 8.7$), 7.82 (d, 2H, $J_o = 8.7$), 7.65 (d, 2H, $J_o = 8.4$), 7.30 (d, 2H, $J_o = 8.4$), 7.31 (s, 1H, OH), 3.91 (s, 2H), 2.34 (s, 3H). Anal. % ($C_{19}H_{16}N_2O_5$) calculated: C 64.77, H 4.58, N 7.95; found C 64.56, H 4.60, N 7.82.

*5.1.2.3. 5-[2-(4′-Chlorobiphen-4-yl)-2-oxoethyl]-5-hydroxy-hexahydropyrimidine-2,4,6-trione (**9**).* 60% Yield, mp > 250 °C ^{1}H NMR δ 10.60 (s, 2H, NH), 7.81 (d, 2H, $J_o = 8.3$), 7.49 (d, 2H, $J_o = 8.3$), 7.40 (d, 2H, $J_o = 8.4$), 7.28 (d, 2H, $J_o = 8.4$), 6.83 (s, 1H, OH), 3.89 (s, 2H). Anal. % ($C_{18}H_{13}ClN_2O_5$) calculated: C 58.00, H 3.52, N 7.51; found C 57.96, H 3.67, N 7.49.

*5.1.2.4. 5-[2-(4′-(Hydroxymethyl)biphen-4-yl)-2-oxoethyl]-5-hydroxy-hexahydropyrimidine-2,4,6-trione (**10**).* 62% Yield, mp > 250 °C ^{1}H NMR δ 11.45 (s, 2H, NH), 8.02 (d, 2H, $J_o = 8.3$), 7.83 (d, 2H, $J_o = 8.3$), 7.71 (d, 2H, $J_o = 8.4$), 7.43 (d, 2H, $J_o = 8.4$), 7.31 (s, 1H, OH), 5.25 (t, 1H, $J = 6.0$, OH), 4.54 (d, 2H, $J = 6.0$), 3.92 (s, 2H). Anal. % ($C_{19}H_{16}N_2O_6$) calculated: C 61.96, H 4.38, N 7.61; found C 61.84, H 4.49, N 7.42.

*5.1.2.5. 5-[2-(4′-Methoxybiphen-4-yl)-2-oxoethyl]-5-hydroxy-hexahydropyrimidine-2,4,6-trione (**11**).* 82% Yield, mp > 250 °C ^{1}H NMR δ 10.78 (s, 2H, NH), 7.63 (d, 2H, $J_o = 8.4$), 7.33 (d, 2H, $J_o = 8.4$), 7.27 (d, 2H, $J_o = 8.8$), 6.74 (s, 1H, OH), 6.68 (d, 2H, $J_o = 8.8$), 3.69 (s, 2H), 3.53 (s, 3H). Anal. % ($C_{19}H_{16}N_2O_6$) calculated: C 61.96, H 4.38, N 7.61; found C 61.64, H 4.45, N 7.53.

*5.1.2.6. 5-[2-(4′-(Trifluoromethoxy)biphen-4-yl)-2-oxoethyl]-5-hydroxy-hexahydropyrimidine-2,4,6-trione (**12**).* 69% Yield, mp > 250 °C ^{1}H NMR δ 11.46 (s, 2H, NH), 8.05 (d, 2H, $J_o = 8.3$), 7.84–7.90 (m, 4H), 7.49 (d, 2H, $J_o = 8.3$), 7.32 (s, 1H, OH), 3.93 (s, 2H). Anal. % ($C_{19}H_{13}F_3N_2O_6$) calculated: C 54.04, H 4.55, N 6.63; found C 53.91, H 4.44, N 6.72.

*5.1.2.7. 5-[2-(4′-(Methylthio)biphen-4-yl)-2-oxoethyl]-5-hydroxy-hexahydropyrimidine-2,4,6-trione (**13**).* 80% Yield, mp > 250 °C ^{1}H NMR δ 11.45 (s, 2H, NH), 8.01 (d, 2H, $J_o = 8.5$), 7.83 (d, 2H, $J_o = 8.5$), 7.71 (d, 2H, $J_o = 8.4$), 7.36 (d, 2H, $J_o = 8.4$), 7.31 (s, 1H, OH), 3.91 (s, 2H), 2.51 (s, 3H). Anal. % ($C_{19}H_{16}N_2O_5S$) calculated: C 59.37, H 4.20, N 7.29; found C 59.58, H 4.21, N 6.89.

*5.1.2.8. 5-[2-(4′-(Methylsulphonyl)biphen-4-yl)-2-oxoethyl]-5-hydroxy-hexahydropyrimidine-2,4,6-trione (**14**).* 65% Yield, mp > 250 °C ^{1}H NMR δ 11.44 (s, 2H, NH), 7.91–8.10 (m, 8H), 7.31 (s, 1H, OH), 3.94 (s, 2H), 3.26 (s, 3H). Anal. % ($C_{19}H_{16}N_2O_7S$) calculated: C 54.80, H 3.87, N 6.73; found C 54.50, H 3.57, N 6.86.

*5.1.2.9. 5-[2-(4′-Acetylbiphen-4-yl)-2-oxoethyl]-5-hydroxy-hexahydropyrimidine-2,4,6-trione (**15**).* 55% Yield, mp > 250 °C (decomp. 235 °C). ^{1}H NMR δ 11.45 (s, 2H, NH), 8.05–8.08 (m, 4H), 7.90–7.93 (m, 4H), 7.31 (s, 1H, OH), 3.94 (s, 2H), 2.61 (s, 3H). Anal. % ($C_{20}H_{16}N_2O_6$) calculated: C 63.16, H 4.24, N 7.37; found C 63.30, H 4.43, N 7.44.

*5.1.2.10. 5-[2-(4′-(N,N-Dimethylaminocarbonyl)biphen-4-yl)-2-oxoethyl]-5-hydroxy-hexahydropyrimidine-2,4,6-trione (**17**).* 62% Yield, mp > 250 °C ^{1}H NMR δ 11.45 (s, 2H, NH), 8.05 (d, 2H, $J_o = 8.3$), 7.88 (d, 2H, $J_o = 8.3$), 7.81 (d, 2H, $J_o = 8.3$), 7.52 (d, 2H, $J_o = 8.3$), 7.32 (s, 1H, OH), 3.93 (s, 2H), 2.98 (s, 3H), 2.94 (s, 3H). Anal. % ($C_{21}H_{19}N_3O_6$) calculated: C 61.61, H 4.68, N 10.25; found C 61.22, H 4.94, N 10.49.

*5.1.2.11. 5-[2-(4′-(Thien-3-yl)phenyl)-2-oxoethyl]-5-hydroxy-hexahydropyrimidine-2,4,6-trione (**18**).* 49% Yield, mp > 250 °C (decomp. 230 °C). ^{1}H NMR δ 11.43 (s, 2H, NH), 8.12 (s, 1H), 7.98 (d, 2H, $J_o = 8.3$), 7.89 (d, 2H, $J_o = 8.3$), 7.66–7.70 (m, 2H), 7.27 (s, 1H, OH), 3.90 (s, 2H). Anal. % ($C_{16}H_{12}N_2O_5S$) calculated: C 55.81, H 3.51, N 8.14; found C 55.52, H 3.87, N 8.42.

*5.1.2.12. 5-[3-(Biphen-4-yl)-2-oxopropyl]-5-hydroxy-hexahydropyrimidine-2,4,6-trione (**19**).* 27% Yield, mp 173–5 °C (decomp. 150 °C). ^{1}H NMR (acetone-d_6) δ 10.24 (s, 2H, NH), 7.60–7.67 (m, 2H), 7.43–7.54 (m, 3H), 7.30–7.37 (m, 3H), 7.16–7.19 (m, 1H), 5.80 (s, 1H, OH), 3.30 (s, 2H), 2.14 (s, 2H). Anal. % ($C_{19}H_{16}N_2O_5$) calculated: C 64.77, H 4.58, N 7.95; found C 64.47, H 4.27, N 7.67.

*5.1.2.13. 5-[1-(Biphen-4-yl)-2-oxopropyl]-5-hydroxy-hexahydropyrimidine-2,4,6-trione (**20**).* 48% Yield, mp > 250 °C ^{1}H NMR (acetone-d_6) δ 10.21 (s, 2H, NH), 7.62–7.71 (m, 4H), 7.44–7.54 (m, 4H), 7.37 (t, 1H, $J_o = 7.5$), 5.72 (s, 1H, OH), 4.88 (s, 1H), 2.05 (s, 3H). Anal. % ($C_{19}H_{16}N_2O_5$) calculated: C 64.77, H 4.58, N 7.95; found C 64.53, H 4.50, N 7.97.

5.2. Biological assays

Inhibitory activities were determined by a fluorimetric assay, where a pro-fluorescing peptide is used as substrate, and the fluorogenic activity of its cleavage product is measured after coincubation of the selected MMP with test compounds.

Assay reagents (Calbiochem) used in the fluorimetric assay were as follows:

- Substrate: Mca-Pro-Leu-Gly-Leu-Dpa-Ala-Arg 25 μM in assay buffer (Calbiochem). This low-fluorescent peptide is cleaved by MMPs to give Mca-Pro-Leu-Gly, which is intensely fluorescent (exc. 340 nm; em. 405 nm).
- Enzymes: pro-MMP-2250 pM; MMP-8 (recombinant catalytic sequence) 500 pM; MMP-9 (recombinant catalytic sequence) 500 pM in assay buffer.
- Assay buffer: tris–HCl 0.1 M, pH 7.5, NaCl 0.1 M, $CaCl_2$ 10 mM, 0.05% v/v BRIJ35, APMA (*p*-aminophenylmercury acetate) 1 mM.

In a typical experiment in 96-well white plate, a solution of inhibitor (50 μL) at the opportune concentration and enzyme (50 μL) was incubated at 25 °C for 30 min; then 10 μL of substrate solution were added and the plate was incubated 3 h at 37 °C. Incubation solutions were quenched with acetic acid (100 μL of 3% soln.) and their fluorescence read with a plate reader spectrometer (Perkin Elmer Victor^3).

Inhibitory activities were calculated against a control and IC_{50} curves, derived from 6 different inhibitor concentrations, extrapolated by means of statistical analysis program Prism (v. 4.0). Each inhibitor concentration was used in triplicate and the experiments run twice. Low active compounds were tested at a single 10 μM concentration (100 μM for compounds **19** and **20**).

5.3. Computational methods

5.3.1. Docking simulations

GOLD (version 5.1), a genetic algorithm based software, was used for the docking study choosing GOLDSCORE and CHEMPLP as

scoring and rescoring functions, respectively. GOLDSCORE is made up of four components that account for protein–ligand binding energy: protein–ligand hydrogen bond energy (external H-bond), protein–ligand van der Waals energy (external vdw), ligand internal van der Waals energy (internal vdw), and ligand torsional strain energy (internal torsion). Parameters used in the fitness function (hydrogen bond energies, atom radii and polarizabilities, torsion potentials, hydrogen bond directionalities, and so forth) were taken from the GOLD parameter file. CHEMPLP is an empirical fitness function optimised for pose prediction and to model the steric complementarity between protein and ligand. It is based on the Piecewise Linear Potential (PLP) that models the attraction as well as repulsion of protein and ligand heavy-atoms and takes into account the distance- and angle-dependent hydrogen and metal bonding terms from ChemScore fitness function. Parameters used in CHEMPLP fitness function were taken by default. Importantly, the use of CHEMPLP permitted to gain a better ranking of docking solutions and comparable results with respect to GOLDSCORE. In the present study, the 3D coordinates of MMP-2 (pdbcode 1HOV), MMP-8 (pdbcode 1I73), and MMP-9 (pdbcode 2OVX) were retrieved from the Protein Data Bank. The target proteins were prepared by adding hydrogen atoms, completing and optimising missing residues, removing water and the cocrystallized molecules by using the Protein Preparation Wizard (Schrödinger 9.2, LLC, New York, NY, 2011). As well known, the histidine side chains cannot normally be placed into the electron density map unambiguously. As a result, the protonation state of such residues was adjusted according to the formation of HB networks that was further confirmed upon visual inspection. The basic amino functional groups were protonated, aromatic amino functional groups were left uncharged and carboxylic groups were considered to be deprotonated. For every protein GOLD was set to generate 10 docking poses per molecule in a sphere of 13 Å radius centred on the centroid atom of cocrystallized ligand.

GOLD was flagged for the automated determination of the coordination geometry around the zinc metal ion. More specifically, virtual coordination points were added at locations where GOLD was missing a coordination site and these coordination points were used as fitting points that could bind to acceptors. In order to determine the coordination geometry, GOLD performs a permuted superimposition of coordination geometry templates onto the coordinating atoms found in the protein. Coordination fitting points were thus generated using the template that gave the best fit in terms of RMSD from the target. The tetrahedral and trigonal bipyramidal coordination geometries were manually specified to allow the docking software to prioritize the Zn metal ion. A visual inspection of solutions demonstrated that our molecules satisfied the structural requisites for a stable coordination with the metal as well as a suitable fitting of the biphenyl fragment into the S_1' subsite.

Following the clues from MD analyses carried out by us in a recent published work [21], which indicate the fluctuation of Arg149 (1HOV numbering) within the time scale of MD simulation, the full side-chain flexibility of such a residue was explicitly considered giving GOLD the option to read alternative allowed rotamers from a library compiled by the most commonly observed side-chain conformations for the naturally occurring amino acids [47].

5.3.2. Pharmaceutically relevant properties predictions

QikProp is an easy-to-use program for a quick and accurate prediction of absorption, distribution, metabolism, and excretion properties (ADME properties). QikProp predicts physically significant descriptors and pharmaceutically relevant properties of organic molecules, either individually or in batches.(QikProp, version 3.4, Schrödinger, LLC, New York, NY, 2011.)

Acknowledgements

The authors gratefully acknowledge the University of Bari "Aldo Moro" (Progetto IDEA – Giovani Ricercatori 2008), the European Commission ("CancerGrid" STREP project, FP VI, Contract No. LSHC-CT-2006-03755) and Regione Puglia (Strategic Project "Neuro-Biotech") for financial support.

Appendix A. Supplementary data

Supplementary data related to this article can be found at http://dx.doi.org/10.1016/j.ejmech.2012.09.036.

References

[1] C.J. Malemud, Front. Biosci. 11 (2006) 1696–1701.
[2] C.M. Overall, O. Kleifeld, Nat. Rev. Cancer 6 (2006) 227–239.
[3] J.E. Rundhaug, J. Cell. Mol. Med. 9 (2005) 267–285.
[4] E.I. Deryugina, J.P. Quigley, Cancer Metastasis Rev. 25 (2006) 9–34.
[5] J.H. Hu, P.E. Van den Steen, Q.A. Sang, G. Opdenakker, Nat. Rev. Drug Discov. 6 (2007) 480–498.
[6] G. Dormán, S. Cseh, I. Hajdú, L. Barna, D. Kónya, K. Kupai, L. Kovács, P. Ferdinandy, Drugs 70 (2010) 949–964.
[7] A.K. Nalla, B. Gorantla, C.S. Gondi, S.S. Lakka, J.S. Rao, Cancer Gene Ther. 17 (2010) 599–613.
[8] B. Govinda Rao, Curr. Pharm. Des. 11 (2005) 295–322.
[9] E. Breuer, J. Frant, R. Reich, Expert Opin. Ther. Patent 15 (2005) 253–269.
[10] M.T. Rubino, M. Agamennone, C. Campestre, P. Campiglia, V. Cremasco, R. Faccio, A. Laghezza, F. Loiodice, D. Maggi, E. Panza, A. Rossello, P. Tortorella, ChemMedChem 6 (2011) 1258–1268.
[11] M.T. Rubino, M. Agamennone, C. Campestre, G. Fracchiolla, A. Laghezza, F. Loiodice, E. Nuti, A. Rossello, P. Tortorella, ChemMedChem 4 (2009) 352–362.
[12] A.R. Folgueras, A. Fueyo, O. Garcia-Suarez, J. Cox, A. Astudillo, P. Tortorella, C. Campestre, A. Gutierrez-Fernandez, M. Fanjul-Fernandez, C.J. Pennington, D.R. Edwards, C.M. Overall, C. Lopez-Otin, J. Biol. Chem. 283 (2008) 9465–9474.
[13] M.T. Rubino, D. Maggi, A. Laghezza, F. Loiodice, P. Tortorella, Arch. Pharm. 344 (2011) 557–563.
[14] J.A. Blagg, M.C. Noe, L.A. Wolf-Gouveia, L.A. Reiter, E.R. Laird, S.P. Chang, D.E. Danley, J.T. Downs, N.C. Elliott, J.D. Eskra, R.J. Griffiths, J.R. Hardink, A.I. Haugeto, C.S. Jones, J.L. Liras, L.L. Lopresti-Morrow, P.G. Mitchell, J. Pandit, R.P. Robinson, C. Subramanyam, M.L. Vaughn-Bowser, S.A. Yocum, Bioorg. Med. Chem. Lett. 15 (2005) 1807–1810.
[15] L.H. Foley, R. Palermo, P. Dunten, P. Wang, Bioorg. Med. Chem. Lett. 11 (2001) 969–972.
[16] J. Wang, C. Medina, M.W. Radomski, J.F. Gilmer, Bioorg. Med. Chem. 19 (2011) 4985–4999.
[17] L.A. Reiter, K.D. Freeman-Cook, C.S. Jones, G.J. Martinelli, A.S. Antipas, M.A. Berliner, K. Datta, J.T. Downs, J.D. Eskra, M.D. Forman, E.M. Greer, R. Guzman, J.R. Hardink, F. Janat, N.F. Keene, E.R. Laird, J.L. Liras, L.L. Lopresti-Morrow, P.G. Mitchell, J. Pandit, D. Robertson, D. Sperger, M.L. Vaughn-Bowser, D.M. Wallera, S.A. Yocum, Bioorg. Med. Chem. Lett. 16 (2006) 5822–5826.
[18] D. Schrigten, H.J. Breyholz, S. Wagner, S. Hermann, O. Schober, M. Schäfers, G. Haufe, K. Kopka, J. Med. Chem. 55 (2012) 223–232.
[19] H.J. Breyholz, M. Schäfers, S. Wagner, C. Höltke, A. Faust, H. Rabeneck, B. Levkau, O. Schober, K. Kopka, J. Med. Chem. 48 (2005) 3400–3409.
[20] M. Piette, B. Evrard, F. Frankenne, P. Chiap, P. Bertholet, D. Castagne, J.-M. Foidart, L. Delattre, G. Piel, Eur. J. Pharm. Sci. 28 (2006) 189–195.
[21] I. Giangreco, G. Lattanzi, O. Nicolotti, M. Catto, A. Laghezza, F. Leonetti, A. Stefanachi, A. Carotti, PLoS One 6 (2011) e25597.
[22] Y. Yan, M.T. Miller, Y. Cao, S.M. Cohen, Bioorg. Med. Chem. Lett. 19 (2009) 1970–1976.
[23] B. Flachner, Z. Lörincz, A. Carotti, O. Nicolotti, P. Kuchipudi, N. Remez, F. Sanz, J. Tóvári, M.J. Szabó, B. Bertók, S. Cseh, J. Mestres, G. Dormán, PLoS One 7 (2012) e35582.
[24] C. Altomare, S. Cellamare, L. Summo, M. Catto, A. Carotti, U. Thull, P.-A. Carrupt, B. Testa, H. Stoeckli-Evans, J. Med. Chem. 41 (1998) 3812–3820.
[25] C. Hansch, A. Leo, Exploring QSAR – Fundamentals and Applications in Chemistry and Biology – ACS Professional Reference Book, American Chemical Society, Washington, DC, 1995.
[26] L. Verdonk, J.C. Cole, M.J. Hartshorn, C.W. Murray, R.D. Taylor, Proteins 52 (2003) 609–623.
[27] C. Knox, V. Law, T. Jewison, P. Liu, S. Ly, A. Frolkis, A. Pon, K. Banco, C. Mak, V. Neveu, Y. Djoumbou, R. Eisner, A.C. Guo, D.S. Wishart, Nucl. Acids Res. 39 (2011) 1035–1041.
[28] C. Hansch, T.E. Klein, Methods Enzymol. 202 (1991) 512–543.
[29] A. Carotti, C. Raguseo, T.E. Klein, R. Langridge, C. Hansch, Chem. Biol. Interact. 67 (1988) 171–184.
[30] A. Carotti, C. Raguseo, F. Campagna, R. Langridge, T.E. Klein, Quant. Struct.–Act. Relat. 8 (1989) 1–10.

[31] A. Carotti, C. Raguseo, C. Hansch, Quant. Struct.–Act. Relat. 4 (1985) 145–149.
[32] A. Carotti, R.N. Smith, S. Wong, C. Hansch, J.M. Blaney, R. Langridge, Arch. Biochem. Biophys. 229 (1984) 112–125.
[33] A. Carotti, M.M. Mueller, J.M. Blaney, R. Langridge, J. Med. Chem. 27 (1984) 1401–1405.
[34] O. Nicolotti, A. Carotti, J. Chem. Inf. Model. 46 (2006) 264–276.
[35] L. Devel, B. Czarny, F. Beau, D. Georgiadis, E. Stura, V. Dive, Biochimie 92 (2010) 1501–1508.
[36] J. Grimm, B.J. Hubs, L.T. Miller, K. Otte, M.P. Siliphaivanh, M. Stanton, G.K. Wilson, D. Witter, H. Zhou, (Merck & Co.), Patent WO2007100657, 2007.
[37] K.J. Wilson, D.J. Witter, J.B. Grimm, P. Siliphaivanh, K.M. Otte, A.M. Kral, J.C. Fleming, A. Harsch, J.E. Hamill, J.C. Cruz, M. Chenard, A.A. Szewczak, R.E. Middleton, B.L. Hughes, W.K. Dahlberg, J.P. Secrist, T.A. Miller, Bioorg. Med. Chem. Lett. 18 (2008) 1859–1863.
[38] O. Nicolotti, I. Giangreco, T.F. Miscioscia, A. Carotti, J. Chem. Inf. Model. 49 (2009) 2290–2302.
[39] O. Nicolotti, T.F. Miscioscia, A. Carotti, F. Leonetti, A. Carotti, J. Chem. Inf. Model. 48 (2008) 1211–1226.
[40] A. Tochowicz, K. Maskos, R. Huber, R. Oltenfreiter, V.R. Dive, A. Yiotakis, M. Zanda, W. Bode1, P. Goettig, J. Mol. Biol. 371 (2007) 989–1006.
[41] H. Brandstetter, F. Grams, D. Glitz, D. Lang, R. Huber, W. Bode, H.W. Krell, R.A. Engh, J. Biol. Chem. 276 (2001) 17405–17412.
[42] P. Pospisil, P. Ballmer, L. Scapozza, G. Folkers, J. Recept. Signal. Transduct. 23 (2003) 361–371.
[43] O. Nicolotti, T.F. Miscioscia, F. Leonetti, G. Muncipinto, A. Carotti, J. Chem. Inf. Model. 47 (2007) 2439–2448.
[44] I. Giangreco, O. Nicolotti, A. Carotti, F. De Carlo, G. Gargano, R. Bellotti, BMC Bioinform. 500 (2010) 1–13.
[45] J.M. Chen, F.C. Nelson, J.I. Levin, D. Mobilio, F.J. Moy, R. Nilakantan, A. Zask, R. Powers, J. Am. Chem. Soc. 122 (2000) 9648–9654.
[46] J. Wang, S. O'Sullivan, S. Harmon, R. Keaveny, M.W. Radomski, C. Medina, J.F. Gilmer, J. Med. Chem. 55 (2012) 2154–6212.
[47] S.C. Lovell, J.M. Word, J.S. Richardson, D.C. Richardson, Proteins 40 (2000) 389–408. 14.